JOURNAL OF GEOPHYSICAL RESEARCH, VOL. 102, NO. D13, PAGES 16,201–16,214, JULY 20, 1997

Chemical reaction rate sensitivity and uncertainty in a two-dimensional middle atmospheric ozone model

Li Chen[1] and Herschel Rabitz
Department of Chemistry, Princeton University, Princeton, New Jersey

David B. Considine and Charles H. Jackman
Atmospheric Chemistry and Dynamics Branch, NASA Goddard Space Flight Center, Greenbelt, Maryland

Jeffrey A. Shorter
Atmospheric and Space Science Division, Mission Research Corporation, Nashua, New Hampshire

Abstract. The NASA Goddard Space Flight Center two-dimensional (2-D) model has been used to study the sensitivity of model ozone concentrations to input chemical reaction rates, and the uncertainty of the model-calculated concentrations. Ozone sensitivity coefficients to changes in chemical reaction rates are defined as logarithmic partial derivatives of the ozone concentration with respect to the chemical reaction rates. These logarithmic derivatives are estimated using a finite difference technique. The ozone sensitivity coefficients to 96 gas phase chemical reactions in the 2-D model show that the ozone concentration is sensitive to the rates of about 25 reactions. The magnitude of the ozone sensitivity coefficients varies from 0.05 to 0.9. The latitude-altitude distributions of the ozone sensitivity coefficients to several reactions are presented. The uncertainty of the model-calculated ozone concentration is evaluated using a guided Monte Carlo (GMC) method from a probability distribution function. The GMC method judiciously combines uncertainty estimates derived from the sensitivity information with Monte Carlo runs of the model. The uncertainty of the model ozone concentration due to uncertainties in gas phase reaction rates is calculated from published chemical rate uncertainties and varies from 10–20% in the lower stratosphere to 30–40% in the mesosphere. Details concerning the GMC method are discussed, and the latitude-altitude distribution of the uncertainty of the model-calculated ozone is presented.

1. Introduction

Two-dimensional (2-D) photochemical models are important tools in the study of stratospheric trace constituents such as stratospheric ozone. They are used to obtain a basic understanding of the chemical, radiative, and transport processes that determine the ozone distribution [e.g., *Douglass et al.*, 1989; *Brasseur et al.*, 1990; *Garcia et al.*, 1992; *Garcia and Solomon*, 1994]. They are also used to predict the response of the atmosphere to various perturbations [*Brasseur and Granier*, 1992; *Schneider et al.*, 1993; *Considine et al.*, 1994], which are sometimes considered in the formulation of industrial regulations. The central role of these models thus requires a clear understanding of the uncertainties associated with the various model predictions.

There are several sources of model uncertainty. First, theoretical models require as input specific values of various parameters, which are estimated or obtained by experiment. The uncertainties in the estimated or measured values of the input parameters produce an uncertainty in the model predictions. Examples of the input parameters are chemical reaction rates, photolysis cross sections, aerosol properties and abundance, and source gas boundary values. In principle, input parameter uncertainties can be propagated through the models, and the output uncertainty due to the input uncertainties can be quantified. In practice, it is sometimes difficult to establish the uncertainty of a model output due to a particular input parameter. Second, stratospheric models are based on a number of simplifying assumptions, each of which could result in a significant deviation of the predicted atmospheric response from the actual response. Examples of this type of uncertainty include the residual circulation formulation, with its parameterization of complex three-dimensional mixing processes in terms of effective diffusion coefficients. In such cases an estimate of the crudeness of the approximation and the sensitivity of the model output to the parameterization can result in a qualitative determination of the model uncertainty. A final source of uncertainty results from important physical processes that are excluded from the model formulation, perhaps because they have not yet been discovered. This type of uncertainty is not quantifiable. However, if model predictions fail to agree with measurements and the discrepancy

[1]Now at Advanced Study Program, National Center for Atmospheric Research, Boulder, Colorado.

Paper number 97JD00702.
0148-0227/97/97JD-00702$09.00

is larger than the model uncertainty resulting from the aforementioned two sources, the likelihood is that important processes have been neglected or that the model formulation itself is suspected. Thus a good understanding of the first two sources of uncertainty results in an ability to address the third.

The evaluation of model uncertainties is closely related to the determination of model sensitivities. If a model displays a large sensitivity to some parameter and the value of that parameter is not well known, then a large uncertainty can result. If the model is sufficiently insensitive to the value of a parameter, then the uncertainty will not be large even if the value of that parameter is not known well.

Three general approaches to the evaluation of the sensitivities and uncertainties in atmospheric models have been employed to varying degrees. The first is referred to as the "hunt and peck" (HP) method because of its reliance on guesswork and trial and error. The HP method consists of guessing what parameters may be important and conducting sensitivity studies to determine if the intuition is correct. This type of uncertainty analysis relying on an individual evaluation of sensitivity coefficients was introduced to the atmospheric chemistry community in a report of the *National Research Council (NRC) Panel on Atmospheric Chemistry* [1976] and was used by *Butler* [1978] and *Stolarski* [1980] in studies of the sensitivity of one-dimensional atmospheric models to various input parameters. It was also employed to examine the uncertainties of trace species inferred from the Limb Infrared Monitor of the Stratosphere (LIMS) satellite measurements of atmospheric constituents [*Kaye and Jackman*, 1986a,b]. The primary disadvantage of the HP approach is that it is not comprehensive. In order to avoid the disadvantage of the HP method in this study, the sensitivity coefficients are evaluated. The ozone sensitivity coefficients to each of the gas phase chemical reaction rates used in the 2-D model are calculated using a finite difference technique.

A second method is a Monte Carlo analysis [*Stolarski et al.*, 1978; *Stolarski and Douglass*, 1986; *Douglass and Stolarski*, 1987.] In this method the value of each input parameter is chosen from a set of possible values distributed in accord with the stated uncertainty in that particular parameter. The model is run many times with different sets of randomly chosen input parameters, and the output is recorded. If enough model runs can be done to build up reliable statistics, this method can produce a good measure of total model output uncertainty due to all of the input parameter uncertainties. Its disadvantage is that the more complicated the model, the more expensive it is to make the necessary runs. Guided Monte Carlo (GMC) analysis is designed to reduce the computational burden of the Monte Carlo method and judiciously combines the results of the sensitivity calculation with the Monte Carlo runs of the model.

A third analysis method is cause and effect analysis [*Andronova and Schlesinger*, 1991]. This method examines the relationships between different model variables, and how a perturbation to a model is transmitted through the model from input to output. The approach is analytical and does not appear to be easily applicable to large computational stratospheric photochemical models.

This paper has two main goals. The first is to calculate a set of coefficients to quantify the sensitivity of the calculated ozone to each of the gas phase chemical reaction rates used in the model, using a finite difference method. The second is to quantitatively estimate the uncertainty in the model prediction of ozone due to the uncertainties in chemical reaction rates. However, the uncertainty of the ozone concentration due to uncertainties in photolysis cross sections and heterogeneous reaction rates is not included in this paper. The ozone sensitivity coefficients to chemical reaction rates are defined and calculated with a 2-D model in section 2. In section 3, the GMC technique is described and the latitude-altitude distribution of the model-calculated ozone uncertainty calculated by the GMC method is presented. Conclusions about the sensitivity and uncertainty of the model calculated ozone to the chemical reaction rates are given in section 4.

2. Sensitivity Study

2.1. Model Description

The NASA Goddard Space Flight Center (GSFC) 2-D model [*Douglass et al.*, 1989; *Jackman et al.*, 1990] is used in this study. This model has been formulated to be computationally economical and so is ideal for the sensitivity and uncertainty studies. The 2-D model extends from the ground up to approximately 92 km with 2 km vertical resolution and from 85°S to 85°N with 10° horizontal resolution. The 46 vertical levels are equally spaced in log pressure. Sixty-five chemical species are considered, of which 30 are transported, including the oxygen, nitrogen, hydrogen, chlorine and bromine families. The remaining species are calculated using photochemical equilibrium assumptions. The species interact through 96 chemical reactions, which are listed in the appendix, and 46 photolytic reactions. The nominal chemical reaction rates are taken from *DeMore et al.* [1992]. Heterogeneous reactions on the surfaces of both stratospheric sulfate aerosols and polar stratospheric clouds are included in the model formulation. The sulfate aerosol surface area concentration distribution used represents background aerosol conditions and was derived from SAGE II satellite observations [*World Meteorological Organization*, 1992]. Type 1 and type 2 polar stratospheric cloud (PSC) surface area densities are calculated using the method described by *Considine et al.* [1994]. Five heterogeneous reactions are considered:

(R1) $N_2O_5 + H_2O \rightarrow 2HNO_3$

(R2) $N_2O_5 + HCl \rightarrow ClONO_2 + HNO_3$

(R3) $ClONO_2 + H_2O \rightarrow HOCl + HNO_3$

(R4) $ClONO_2 + HCl \rightarrow Cl_2 + HNO_3$

(R5) $HOCl + HCl \rightarrow Cl_2 + H_2O$

Reactions on sulfate aerosols are treated following *Hanson and Ravishankara* [1994]. Sticking coefficients for (R1) on sulfate aerosol, and the other reactions on type 1 and 2 PSCs are taken from *DeMore et al.* [1992]. An adjustment to account for relative humidity is made to the sticking coefficients for (R3), (R4), and (R5) on type 1 PSCs, as suggested by *Tabazadeh and Turco* [1993] and *Hanson and Ravishankara* [1993].

A residual mean circulation is calculated following *Dunkerton* [1978]. The heating rates of *Dopplick* [1974, 1979] are used between 100 mbar and the ground, while Rosenfield et al. (1987) heating rates are used above 100 mbar. The temperature field is a 4-year average (1979–1982) of the National Meteorological Center (NMC) data up to 0.4 mbar and

CIRA (1972) temperature data above 0.4 mbar. The values of the vertical diffusion coefficient K_{zz} are fixed in the middle atmosphere at 2×10^3 cm^2s^{-1}. In the troposphere, K_{zz} decreases with increasing altitude to the stratospheric value from the value of 1×10^5 cm^2s^{-1} at the ground. The K_{yy} values are calculated to be consistent with the residual circulation [*Fleming et al.*, 1995]. Operator splitting is used to separate the chemical and advective operators. Advection is calculated using the second moment conserving scheme of *Prather* [1986].

2.2. Definition of Ozone Sensitivity Coefficient

The sensitivity method explored here is to isolate a single model output variable such as the ozone concentration ($[O_3]$) and study its response to a single input variable such as a chemical reaction rate (k_i) assuming all other inputs constant. The sensitivity coefficient S_i of the ozone concentration at different latitudes and altitudes to variations in the reaction rate k_i is defined by

$$S_i = \frac{\partial \ln[O_3]}{\partial \ln k_i} = \frac{k_i}{[O_3]} \frac{\partial [O_3]}{\partial k_i}. \quad (1)$$

In this paper these logarithmic derivatives are estimated using a finite difference technique. The ozone sensitivity coefficient is calculated by

$$S_i = \frac{\ln[O_3]' - \ln[O_3]}{\ln k_i' - \ln k_i} = \frac{\ln[O_3]' - \ln[O_3]}{\ln f_i}, \quad (2)$$

where $[O_3]$ and $[O_3]'$ are the model calculated ozone concentration for the nominal reaction rate k_i and for the perturbed rate k_i' and $f_i = k_i'/k_i$. The sensitivity coefficient S_i is a dimensionless number indicating how the ozone concentration responds to a change in one of the chemical reaction rates. Since the sensitivity coefficient is essentially the ratio of the fractional change in ozone to a fractional change in a chemical reaction rate, a sensitivity coefficient of 0.1 would imply a 1% change in ozone for a 10% change in the value of a reaction rate. Normally, the magnitude of species sensitivity coefficients varies from 0 to 1. A sensitivity coefficient of 1 or larger implies that the species is highly sensitive to the reaction rate. If the coefficient is less than 0.05, the species is quite insensitive to the reaction rate. It should be noted that the sensitivity coefficient rigorously applies only for relatively small variations around the nominal reaction rates and that the significance of a small or large sensitivity coefficient for a particular reaction rate should not be overinterpreted. For instance, it is not necessarily true that a reaction having a very small sensitivity coefficient is unimportant and can be eliminated from the reaction rate set. It is possible for ozone concentrations to be insensitive to small changes in a reaction around its nominal rate and still change by a large amount when that reaction rate is set to zero.

2.3. Model Calculation and Results

Stolarski [1980] used a one-dimensional model to calculate the ozone sensitivity coefficients to chemical reaction rates and found that the model calculated ozone was highly sensitive to the reactions $N_2O+O(^1D) \rightarrow 2NO$, $ClO+O \rightarrow Cl+O_2$, and $OH+HO_2 \rightarrow H_2O+O_2$. We have used these three reactions and the other chemical reactions that are important to the odd oxygen destruction (e.g., $O+O_3 \rightarrow 2O_2$, $OH+O_3 \rightarrow HO_2+O_2$, $HO_2+O_3 \rightarrow OH+2O_2$, $NO_2+O \rightarrow NO+O_2$, $OH+O \rightarrow H+O_2$, and $HO_2+O \rightarrow OH+O_2$) to determine an appropriate value for the perturbed reaction rate k_i' in equation (2). We also calculate using these reactions the additional model integration time needed to obtain a new steady state for the perturbed value of k_i'. The ozone sensitivity coefficients for these reactions calculated using $k_i' = 1.05k_i$, $1.1k_i$, and $1.3k_i$ do not show any appreciable differences for the three different k_i', but the altitude profile of the ozone sensitivity for $k_i' = 1.05k_i$ starts to become unsmooth, indicating numerical instability. This suggests that $k_i' = 1.1k_i$ is a reasonable value to adopt to calculate the ozone sensitivity coefficient. We do not need to have a close approximation to the limiting value of the sensitivity coefficient as k_i' approaches k_i in order to obtain the goal of this study, which is to learn what the sensitivity coefficients say about the response of ozone to the various reaction rates, not to get as close an approximation to the logarithmic partial derivatives of ozone to the model reaction rates. We then ran the 2-D model for 2, 8, and 10 years from steady state using the perturbed value $k_i' = 1.1k_i$, for each reaction rate and found that the model reached a new steady state for this small perturbation of k_i after 2 years. Since $k_i' = 1.1k_i$, and 2-year model integration are appropriate for the reactions which have relatively large imparts on the calculation of the ozone concentration, it should be reasonable for other reactions. Therefore the 2-D model is first run for 20 years to a seasonally repeating steady state and continually run for another 2 more years from the steady state for the nominal k_i taken from *DeMore et al.*, [1992] and for the slightly perturbed k_i' ($k_i' = 1.1k_i$). The latitude-altitude distributions of the ozone sensitivity coefficients are then calculated from the model output using (2). Although the sensitivity coefficients vary with season, for the purposes of this paper it is sufficient to intercompare the sensitivity coefficients at equinox, to avoid the added complication of polar night conditions. The sensitivity coefficients in March are very similar to the results in September, so we present zonal mean plots of the sensitivity coefficients in September below.

The model ozone concentration shows a substantial sensitivity to about 25 of the 96 gas phase reactions included in the 2-D model. By substantial we mean that the sensitivity coefficient exceeds 0.05 somewhere in the model domain. Table 1 lists the chemical reactions to which the ozone concentration is most sensitive. Column 1 numbers the reaction for later reference, column 2 is the reaction, column 3 gives the range of the maximum absolute values of the ozone sensitivity coefficient, and columns 4 and 5 are the altitude and latitude location of this maximum.

Table 1 shows that the ozone concentration is most sensitive to k_1 and k_2 in the upper mesosphere and to k_5 and k_6 in the middle and lower mesosphere. In the upper stratosphere the ozone concentration is more sensitive to k_8 and k_9 than to other reactions. In the middle stratosphere ozone is sensitive to k_{12} at low latitudes and to k_{15} at high latitudes.

Figure 1a shows the ozone sensitivity coefficient to chemical reaction 1 in Table 1. The ozone concentration is most sensitive to k_1 in the upper stratosphere and the mesosphere compared with other reactions. Since k_1 converts atomic

Table 1. Chemical Reactions to Which the Ozone Density is Most Sensitive

	reaction	max. range of S_i	location	
			altitude, km	latitude*
1	$O + O_2 + M \rightarrow O_3 + M$	0.7–0.9	60–80	
2	$HO_2 + O \rightarrow OH + O_2$	-0.6– -0.7	70–80	
3	$H + O_2 + M \rightarrow HO_2 + M$	-0.2– -0.3	75–80	60°S–75°N
4	$H + O_3 \rightarrow OH + O_2$	-0.1– -0.3	70–80	
5	$O + OH \rightarrow H + O_2$	-0.3– -0.4	60–70	
6	$HO_2 + OH \rightarrow O_2 + H_2O$	0.3–0.4	55–70	
7	$H_2O + O(^1D) \rightarrow 2OH$	-0.2	40–60	60°S–75°N
8	$HCl + OH \rightarrow Cl + H_2O$	-0.25– -0.35	40–50	
9	$Cl + O_3 \rightarrow ClO + O_2$	-0.2	40–50	
10	$O + O_3 \rightarrow 2O_2$	-0.1– -0.2	40–50	
11	$Cl + CH_4 \rightarrow HCl + CH_3$	0.1	45	
12	$NO + O_3 \rightarrow NO_2 + O_2$	-0.2	35–45	40°S–40°N
13	$ClO + O \rightarrow Cl + O_2$	-0.1– -0.3	35–45	
14	$N_2O + O(^1D) \rightarrow 2NO$	-0.1– -0.3	30–40	
15	$NO_2 + O \rightarrow NO + O_2$	-0.4– -0.5	25–35	75°S–60°S

* The latitudinal range is from 75°S to 75°N if it is not specified.

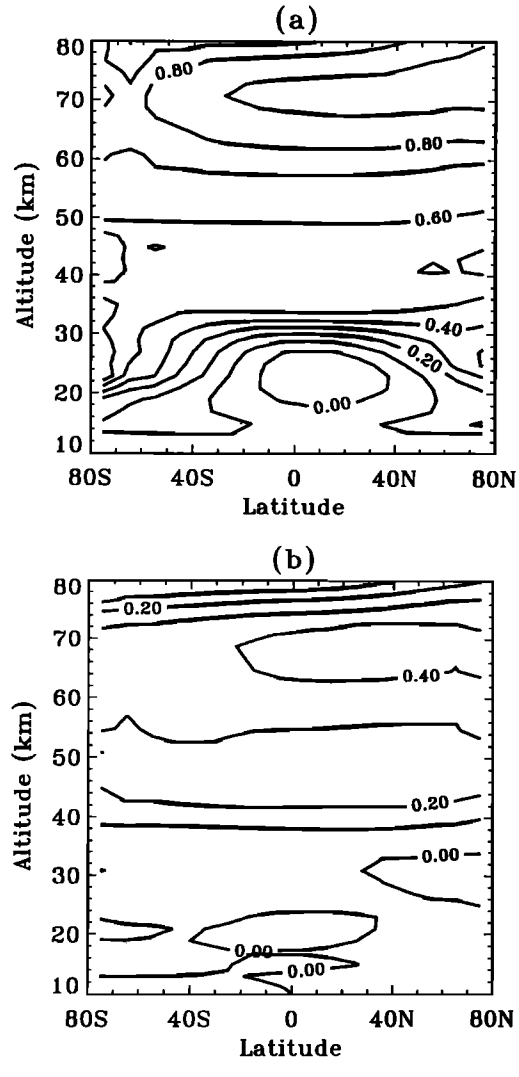

oxygen into ozone, ozone will increase by increasing the rate k_1 except in the small negative area of low magnitude around 20 km over the low latitudes. These positive sensitivity coefficients have a maximum of 0.9 around 65–75 km. The small area of the negative ozone sensitivity is a consequence of the larger ozone increases at higher levels shielding lower levels from solar UV (i.e., a nonlocal self-healing effect). Above 30 km the latitudinal dependence of the ozone sensitivity to Reaction 1 is almost negligible because chemistry is more dominant than dynamics in the ozone distribution. Below 30 km the ozone sensitivity to k_1 at high latitudes becomes positive, while it is negative at low latitudes. This is primarily caused by the latitudinal variation of solar zenith angle and transport. Poleward motion in the middle stratosphere and downward motion at high latitudes move the increased ozone at 25–30 km over low latitudes, brought about by increases in the rate of k_1, to the lower levels at high latitudes. We calculated the horizontal transport of ozone due to advection and diffusion for the cases of k_1 and $1.1k_1$ and found that the horizontal transport for the latter case is increased by about 10% around 30 km in the southern high latitudes. The increase at northern high latitudes is smaller.

A large ozone sensitivity coefficient is also found for k_6 in the upper stratosphere and the mesosphere and this result is shown in Figure 1b. The ozone concentration above about 40 km increases with an increase in the rate of k_6. An enhancement of Reaction 6 destroys more OH and HO_2 with a subsequent reduction of the destruction of the odd oxygen due to HO_x. This effect peaks near 68 km, where the ozone loss due to HO_x reaches a maximum. The sensitivity to k_6 below 30 km is negligible.

Figure 1. The latitude-altitude distribution of the ozone sensitivity coefficient to the chemical reactions (a) $O+O_2+M \rightarrow O_3+M$ (k_1) and (b)$HO_2+OH \rightarrow O_2+H_2O$ (k_6) in September.

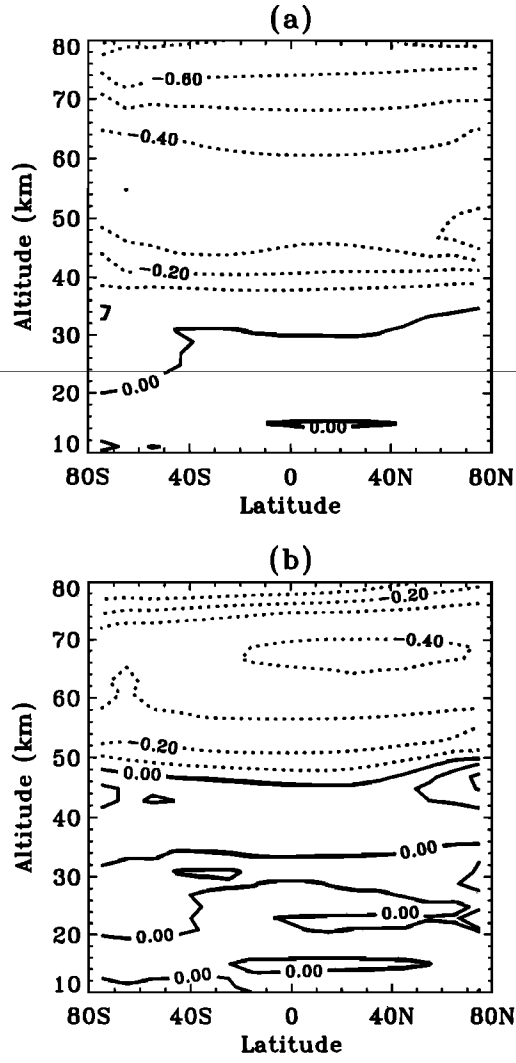

Figure 2. The same as Figure 1 except to the reactions (a) $HO_2+O \rightarrow OH+O_2$ (k_2) (b) $O+OH \rightarrow H+O_2$ (k_5).

Figures 2(a) and (b) show the ozone sensitivity coefficients to k_2 and k_5. Both of these reactions 2 and 5 in Table 1 involving hydrogen free radicals represent a very rapid loss process for atomic oxygen and reduce ozone in the mesosphere. The negative maxima of the ozone sensitivity coefficients to k_2 and k_5 are -0.7 around 80 km and -0.4 around 68 km. In the narrow region 40–50 km, the sensitivity to k_5 becomes positive because k_5 destroys OH with a subsequent reduction of the conversion of the inactive chlorine bound HCl to the active chlorine Cl by OH (see, e.g., reaction 8 in Table 1). The region of the positive ozone sensitivity to k_5 is collocated with a region of decreased active chlorine. Thus enhancing k_5 decreases the ozone destruction due to ClO_x and increases ozone at altitudes of 40–50 km. Because of the latitudinal dependence of the active chlorine (the abundance of active chlorine (ClO and Cl) is higher at high latitudes than at low latitudes), this positive sensitivity coefficient has a larger value at high latitudes than at low latitudes.

The ozone concentration displays a sensitivity to k_3 and k_4 above 70 km and is decreased by the enhancement of these rates. This is because atomic hydrogen starts to become important in ozone destruction above 70 km. The values of the sensitivity coefficients to k_3 and k_4 are about -0.4 and -0.3 at 80 km. The ozone concentration also shows a negative sensitivity to k_7 at altitudes between 35 and 70 km. Its maximum is about -0.25 at 50 km. The oxidation of water vapor by $O(^1D)$ is the primary source of OH below 60 km. In addition, as was pointed out before, more OH increases the conversion of HCl to Cl and destroys more ozone by increasing chlorine catalysis in addition to the direct effects of changes in HO_x catalysis of O_3.

Figures 3a and 3b show that the ozone concentration decreases and increases with the increase in the chemical reaction rates k_8 and k_{11}, respectively. The increased in k_8 increases the conversion of HCl to Cl and causes greater ozone destruction, while k_{11} has the opposite effect. The ozone concentration is more sensitive to k_8 at high latitudes than at low latitudes because at an altitude of 40–50 km, the fraction of ozone loss due to chlorine chemistry is largest at high latitudes.

Figures 4a and 4b display the latitude-altitude distributions of the ozone sensitivity coefficients to k_{15} and k_{12}. These cycles catalyze the destruction of odd oxygen; therefore the ozone concentration decreases with increases in their rates. The ozone concentration displays a substantial sensitivity to the NO_x cycle (reactions 12 and 15 in Table 1) throughout the stratosphere and maximizes at 35–45 km because the NO_x cycle is most efficient

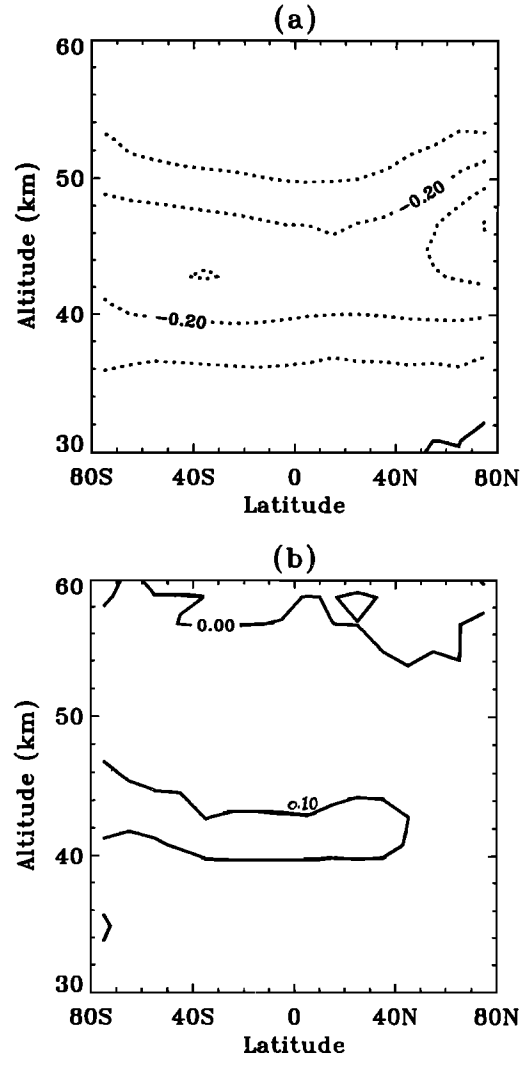

Figure 3. The same as Figure 1 except to the reactions (a) $HCl+OH \rightarrow Cl+H_2O$ (k_8) (b) $Cl+CH_4 \rightarrow HCl+CH_3$ (k_{11}).

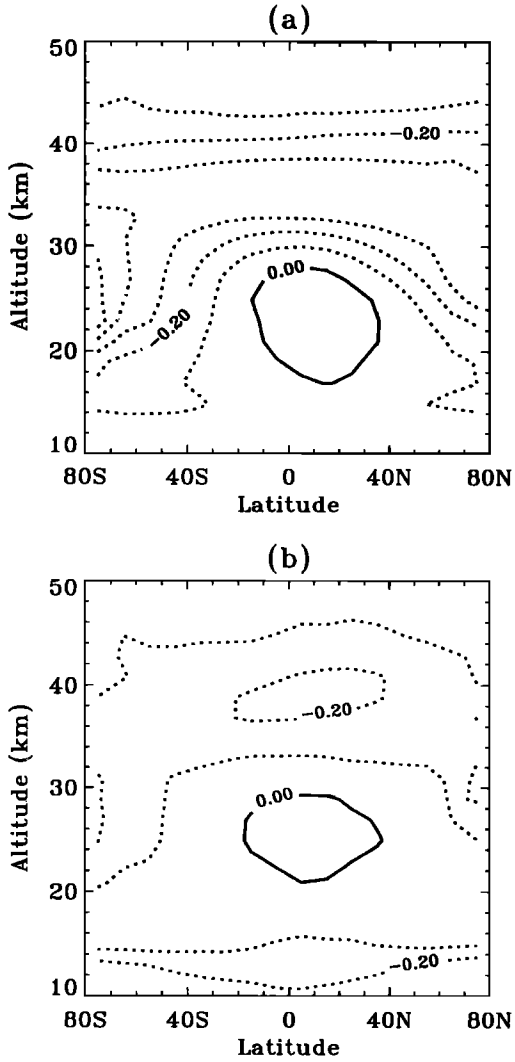

Figure 4. The same as Figure 1 except to the reactions (a) $NO_2+O \rightarrow NO+O_2$ (k_{15}) (b) $NO+O_3 \rightarrow NO_2+O_2$ (k_{12}).

there. The positive ozone sensitivity coefficient to k_{15} in a small area over the tropics at altitudes 20–30 km is due to the effect of ozone self-healing. The ozone sensitivities to k_{12} and k_{15} are independent of latitude in the upper stratosphere, but in the middle stratosphere they show very strong latitudinal dependence stemming from the poleward motion in the middle stratosphere and downward motion at high latitudes as discussed above. Since the ClO_x cycle (reactions 9 and 13 in Table 1) is quite effective in the upper stratosphere and is inhibited at lower altitudes by conversion of ClO to $ClONO_2$ and HCl, the ozone concentration is most sensitive to the ClO_x reactions in the upper stratosphere. The latitude-altitude distributions of the ozone sensitivity coefficients to k_9 and k_{13} are shown in Figures 5a and 5b. The sensitivity coefficients to k_9 and k_{13} show latitudinal dependencies very similar to those of the active chlorine distributions.

The ozone concentration also shows a negative sensitivity to k_{14} and k_{10}. In the stratosphere, NO is produced mostly by reaction of N_2O with an excited oxygen atom in the (^1D) state. The negative maximum of the ozone sensitivity to k_{14} is about -0.2 at 35 km. Reaction 10 directly destroys the odd oxygen and the ozone sensitivity to this reaction is about -0.15 near 50 km.

The aforementioned chemical reactions to which the ozone concentration displays a relatively large sensitivity are all known to be quite important for the stratospheric and mesospheric ozone chemistry. Thus these results both quantify and spatially locate the important chemical processes in the stratosphere and the mesosphere that determine the ozone distribution.

The ozone sensitivity coefficients to the following reactions are less than 0.05.

$$OH + O_3 \rightarrow HO_2 + O_2,$$

$$O(^1D) + M \rightarrow O + M,$$

$$ClO + NO \rightarrow Cl + NO_2,$$

$$ClO + NO_2 + M \rightarrow ClONO_2 + M.$$

Ozone is sensitive to the reactions $HO_2+O_3 \rightarrow OH+2O_2$ and $HO_2+NO \rightarrow OH+NO_2$ only below 15 km. This study also shows that ozone is sensitive to the reaction $OH+NO_2+M \rightarrow HNO_3+M$ only at high latitudes between 20 and 30 km. In contrast, *Stolarski* [1980] used a 1-D model representative of mid-

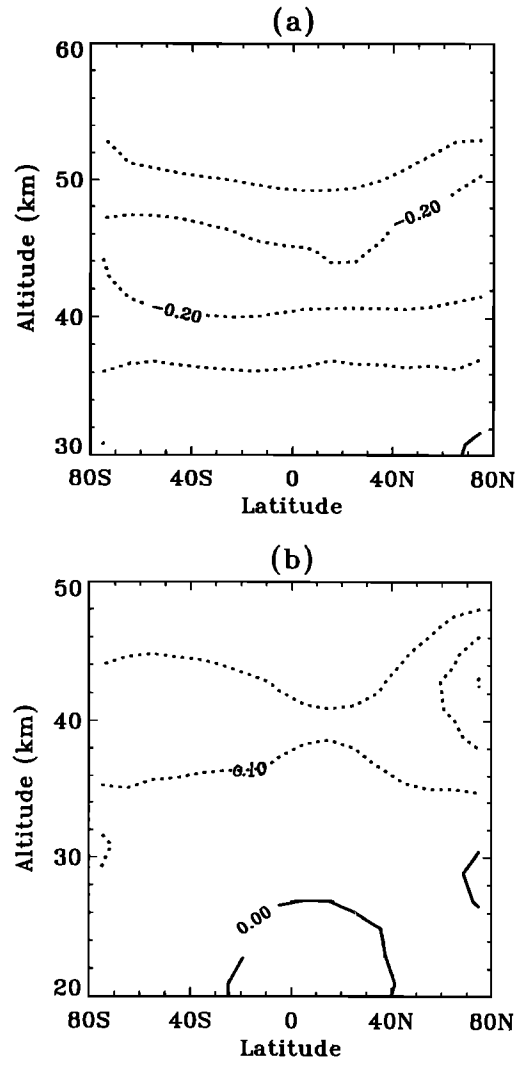

Figure 5. The same as Figure 1 except to the reactions (a) $Cl+O_3 \rightarrow ClO+O_2$ (k_9) (b) $ClO+O \rightarrow Cl+O_2$ (k_{13}).

latitude chemical processes and obtained a large sensitivity coefficient (about 0.25) to this reaction. This difference could be caused by the neglect of the horizontal transport in the 1-D model and also by the recent changes in rate constants which have shifted the dominance of ozone chemistry in the lower stratosphere from NO_x cycle to HO_x cycle. We also find that the sensitivity coefficients for the chemical reactions involving bromine species are small (<0.05). We have also recalculated the ozone sensitivity coefficients with an additional pathway to HCl from the reaction of ClO+OH included in the GSFC 2-D model reaction set. This reaction path has been proposed by several research groups as a possible solution to the O_3 underestimate and ClO overestimate common to stratospheric photochemistry models in the upper stratosphere [*McElroy and Salawitch*, 1989; *Chandra et al*, 1993; *Minschwaner et al.*, 1993]. The value of the ozone sensitivity coefficient to this pathway at a 7% branching yield, as suggested by *Chandra et al* [1993], is about 0.1–0.2 at altitudes of 40–50 km from middle to high latitudes. This pathway increases the inactive chlorine reservoir (HCl) and decreases the active chlorine (ClO) and consequently increases ozone. Therefore the ozone concentration displays a positive sensitivity to this channel in the region where ClO_x plays an important role in the ozone destruction. Including this channel in the 2-D model reduces the ozone sensitivity to the reactions involving ClO_x (reactions 8,9,11,13, and 15) by about 0.05–0.1 at altitudes of 40–50 km, and increases the ozone sensitivity to reaction 1 by about 0.1 at these levels.

3. Guided Monte Carlo Analysis

3.1. Description of Technique

As described in section 1, Monte Carlo analysis randomly selects new sets of input chemical reaction rates $\{k_i'\}$ from each rate's probability distribution which is formed in accordance with the *DeMore et al.* [1992] rate parameter 1σ uncertainties for the temperature of 298 K. The effects of the temperature dependence of uncertainties in the rate constants on the calculated ozone concentration will be discussed in section 3.2. The 2-D model is repeatedly run with each sets of chemical reaction rates. After many model runs (typically about 1000–2000, [see *Stolarski*, 1980], a probability distribution of the ozone concentration can be generated for any model location and time of year. This distribution represents the uncertainty in the model calculated ozone due to uncertainties in all of the input chemical reaction rates. The complete Monte Carlo analysis is very expensive to apply to 2-D models because the large number of model runs requires exceptionally long computational time.

The sensitivity coefficients discussed in the previous section can also be used to estimate both the value of the model ozone concentration for the new set of reaction rates and its uncertainty due to reaction rate uncertainties. This can be done if we assume that the dependence of the model-calculated ozone on chemical reaction rates is linear. The change of the ozone concentration can be estimated by

$$\varepsilon = \sum_{i=1}^{96} S_i(\ln k_i' - \ln k_i), \qquad (3)$$

where $\{k_i'\}$, i=1, 2,...,96, is the new sampled reaction rate and ε is simply the estimated fractional change in ozone that would result from running the model with the new rate set $\{k_i'\}$. The uncertainty can be calculated by

$$U_i = \delta[O_3]/[O_3] = \delta \ln[O_3]. \qquad (4)$$

where U_i is the fractional uncertainty in the calculated ozone due to the reaction rate k_i.

By using the definition of sensitivity (equations (1) and (2)),

$$U_i = S_i \delta \ln k_i = S_i(\ln k_i' - \ln k_i) = S_i \ln f_i, \qquad (5)$$

Here each k_i' is chosen so $\delta \ln k_i'$ quantifies the fractional uncertainty f_i in k_i. The total uncertainty (U_{total}) can be estimated by a root-mean-square sum, i.e.,

$$U_{total} = \sqrt{\sum_i U_i^2} = \sqrt{\sum_i (S_i \ln f_i)^2}. \qquad (6)$$

The uncertainty f_i in the rate constants of the two-body reactions for the temperature of 298 K is taken from *DeMore et al.* [1992]. An estimate of the uncertainties at any given temperature is obtained from

$$f(T) = f(298)\exp\left|\frac{\Delta E}{R}\left(\frac{1}{T} - \frac{1}{298}\right)\right|. \qquad (7)$$

The f_i values for the three-body reactions are estimated by simply calculating the lowest possible rate and the highest possible rate using the uncertainties of k_0 and n from *DeMore et al.* [1992] for the low pressure limit, where k_0 and n are the two parameters in the formula of the three body reaction rates.

Compared with the Monte Carlo method, the estimate of the ozone uncertainty based only on the sensitivity results is very economical. Its expense is little more than the cost of calculating the ozone sensitivity coefficients, which requires a single run for each reaction rate, or 96 model runs. However, unlike the Monte Carlo technique, the accuracy of the estimate depends completely on an assumption of a linear relationship between the output ozone and the input reaction rates.

In order to avoid the deficiencies of both the Monte Carlo method and the sensitivity coefficient estimation (SCE) procedure described above (equation (3)) we employed the guided Monte Carlo technique [*Shorter and Rabitz*, 1997]. The GMC method judiciously combines the information of efficient sensitivity analysis with the Monte Carlo runs of the model. Figure 6 is a logic flow diagram indicating how the GMC method is designed. Random sampling of the reaction rates is still maintained, but the model is not run with all the chosen rate sets. The model is run only when a selected rate set is predicted by the SCE procedure to have a relatively large impact on the calculated ozone. The GMC method thus significantly reduces the total computational time. The impact of each new rate set on the calculated ozone is estimated by using equation (3). If the new set of chemical reaction rates is estimated to cause a small change in the ozone concentration from its nominal value, ε will be a good estimate of the fractional change in ozone, and the ozone concentration is predicted with the sensitivity results. If the new set causes a large change in the ozone concentration, ε will not likely be a good estimate, and the ozone concentration should be determined by rerunning the model. The value of $|\varepsilon|$ above

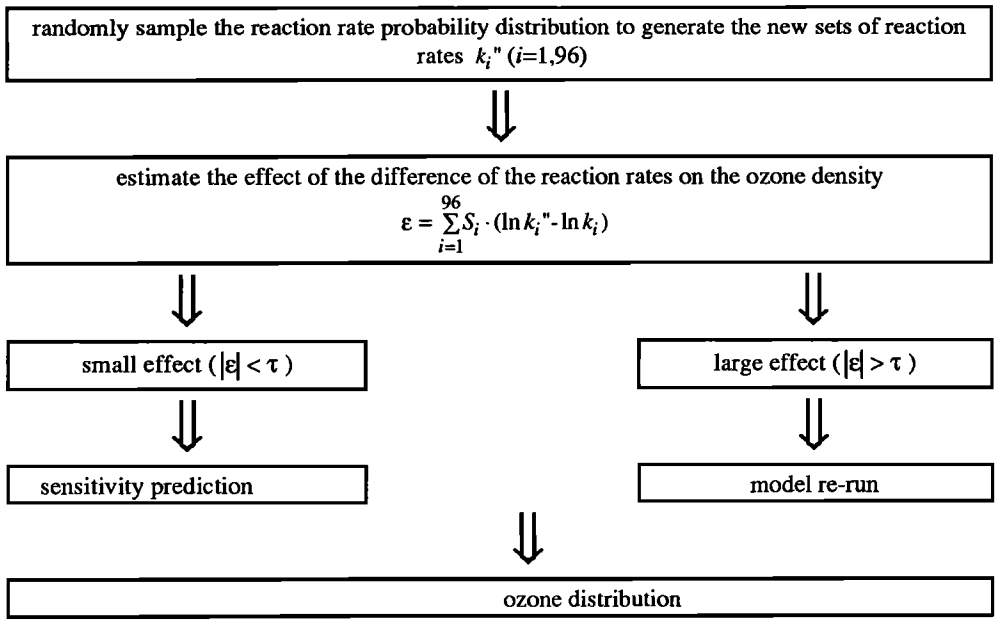

Figure 6. The logic flow diagram for the GMC method.

which the model is run, τ, is chosen empirically. It is generally most economical to start with a large τ value (i.e., ozone concentration from sensitivity analysis alone) and systematically decrease it to get the converged value of ozone concentration.

3.2 Model Calculation and Results

We selected 1000 sets of randomly chosen chemical reaction rates from each rate's probability distribution based on the *DeMore et al.* [1992] chemical rate 1 σ uncertainties $\{f_i\}$ for the temperature of 298 K. The f_i is used to establish the width of the probability distribution of the reaction rate k_i which is used to select a possible value for the ith reaction rate. The random selection of the reaction rates from their probability distributions can only be done for one temperature. Otherwise, the reaction rate would vary randomly from location to location in the model. For each reaction rate set, we calculate ε in September using equation (6). Since it is more likely inaccurate to derive the ozone concentration from the sensitivity information in the area where the large values of $|\varepsilon|$ are located, we compare the maximum of the absolute value of ε over all latitudes and altitudes with the chosen τ. If this maximum of $|\varepsilon|$ is smaller than the chosen τ, the ozone concentration over all the area will be calculated from the sensitivity results; if the maximum is larger, the model will be rerun to determine the ozone concentration over all latitudes and altitudes. The choice of τ determines the number of cases requiring a model run and the number of cases for which the sensitivity results can be used. We tested values of τ ranging from 0.5 to 1, as shown in Table 2.

For different τ the ozone concentrations at all latitudes and altitudes are calculated for the 1000 sets of randomly selected chemical reaction rates either by using the sensitivity results or by rerunning the model (see, Table 2). The ozone mean and the standard deviation are calculated from the results of these 1000 cases for different latitudes and altitudes. Plots of the ozone mean and its standard deviation at different locations with respect to τ showed that these statistical measures are satisfactorily converged at $\tau = 0.5$ (i.e., further reductions in τ will not change the mean and standard deviation of ozone). Therefore the following results are for $\tau = 0.5$. Table 2 shows that the GMC procedure requires 307 model runs. Combined with the 96 runs necessary to calculate the sensitivity coefficients, this represents over a factor of 2 reduction in the total number of runs.

The normalized distributions of the ratio of the ozone concentration for each GMC run to its nominal value are shown in Figure 7. The figure shows the distributions at latitudes of 5° N, 45° N, and 75° N and altitudes of 20 km, 40 km, and 60 km. The probability distributions at other latitudes and altitudes are very similar to these. All of the distributions show that in the center the probability built up by the sensitivity calculations is much larger (about 5–6 times larger) than that by the Monte Carlo runs of model, while in the tails they are comparable. Therefore the central part of the ozone probability distribution tends to be built up by information from the

Table 2. Required Monte Carlo Model Runs and Sensitivity Analysis

τ	Model runs	Sensitivity Analysis
1.0	6	994
0.9	7	993
0.8	26	974
0.7	71	929
0.6	123	877
0.5	307	693

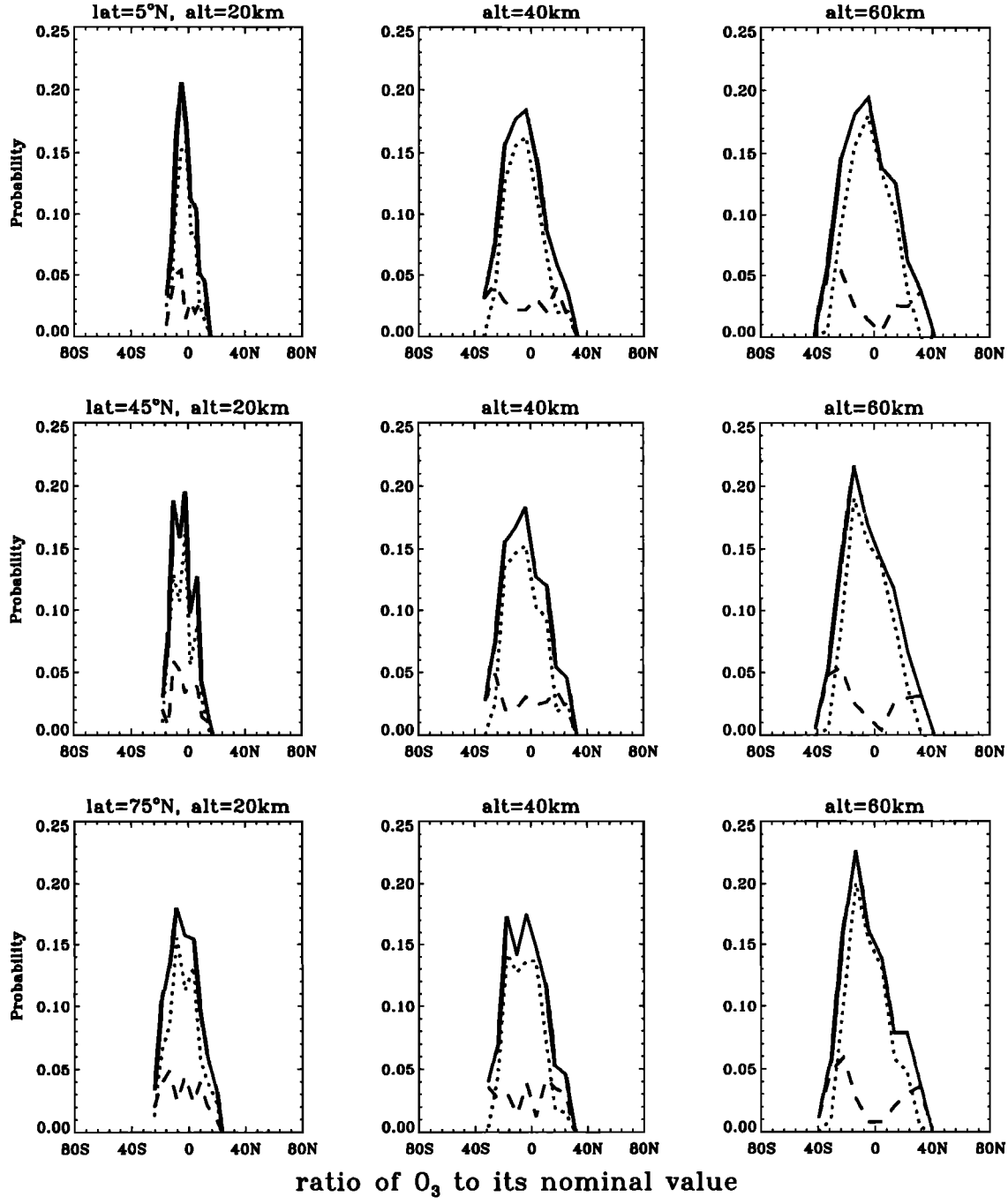

Figure 7. The ozone probability distribution (solid line) with respect to the ratio of the calculated ozone density over its nominal value for the selected latitudes (5°N, 45°N, and 75°N) and altitudes (20, 40, and 60 km). The dotted and dashed lines are partial distributions derived from sensitivity analysis and model re-runs, respectively. The full distribution is a sum of the latter quantities.

sensitivity analysis, and the wings are controlled by the MC runs of model. This behavior is consistent with the GMC logic [*Shorter and Rabitz*, 1997] presented in section 3.1. Figure 7 also shows that the probability distributions broaden at higher altitudes and the broadness is relatively independent of latitudes.

Figure 8a shows the nominal value of the ozone mixing ratio in September, and Figure 8b is the mean value of the ozone concentration calculated by using the GMC method for the case of $\tau = 0.5$. Their latitude-altitude distributions are very similar although the nominal value is slightly lower (by $\lesssim$ 5%)than the mean value above 50 km. Compared with satellite observations, the ozone distribution is quite reasonable obtained by the GSFC nominal model [*WMO*, 1994; *Fleming et al.*, 1995] or the GMC approach using the recommended reaction rates from *DeMore et al.* [1992].

An interesting issue is whether the ozone distribution function exhibits an asymmetry with respect to the nominal value. The uncertainty of the model ozone prediction was estimated by calculating the right and left hand standard

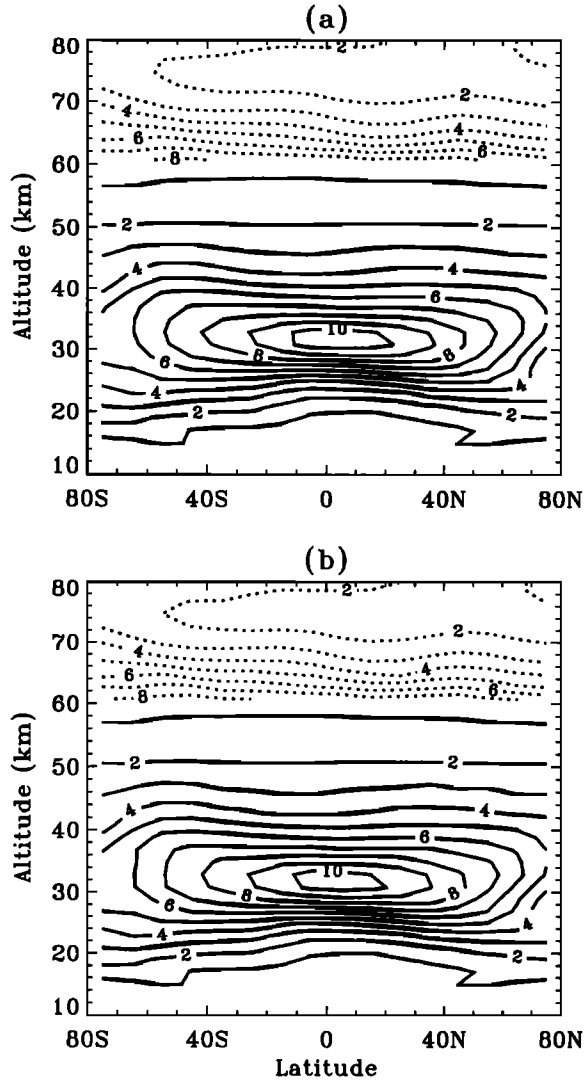

Figure 8. (a) The nominal value of the ozone mixing ratio (part per million by volume, ppmv) calculated by the GSFC 2-D model using the recommended reaction rates from *DeMore et al.* [1992]. (b) The mean of the ozone mixing ratio (ppmv) calculated by using the GMC method. The dotted lines represent the ozone mixing ratio multiplied by 10.

deviations from the GMC results for different latitudes and altitudes. They are shown in Figures 9a and 9b as percent relative to nominal value. The right side value is larger than the left one, especially at higher altitudes as is consistent with the results in Figure 8. In the middle stratosphere the uncertainty of the ozone concentration due to uncertainties in chemical reaction rates is at least 5–25%, and in the mesosphere it is 30–35%. In the mesosphere the latitudinal dependence of the standard deviation is almost negligible, but in the lower stratosphere the standard deviations at high latitudes are larger than those at low latitudes. This latitudinal dependence is primarily due to the latitudinal dependence of the ozone sensitivities resulting from the dynamical impact and the latitudinal variation of solar zenith angle.

For simplicity, these 1σ uncertainties in chemical reaction rates for the temperature of 298 K are used for generating reaction rate sets. Since 298 K is higher than the typical temperature of the stratosphere and the mesosphere, the real ozone uncertainty due to uncertainties in chemical reaction rates is somewhat larger than these calculations. In order to see the impact of these simplifications on the estimate of the ozone uncertainty, equation (6) is used for T=298 K and for the temperature field adopted in the 2-D model. The results are shown in Figures 10a and 10b. The calculated ozone uncertainty due to the rate uncertainties is generally larger for the 2-D model adopted temperature than for the temperature of 298 K. For the realistic atmosphere temperature the uncertainty in the ozone concentration due to uncertainties in the gas phase reaction rates increases up to 10–20% in the lower and middle stratosphere, 20–30% in the upper stratosphere and 30–40% in the mesosphere. The ozone uncertainty derived here does not include that due to uncertainties in photolysis cross sections and in heterogeneous reactions. These factors should be explored in future studies.

Finally, in those cases with $|\varepsilon| > \tau$, we can obtain both a model-calculated ozone distribution and a predicted ozone distribution using the sensitivity coefficient estimation procedure. If the ozone chemical system is basically linear, the

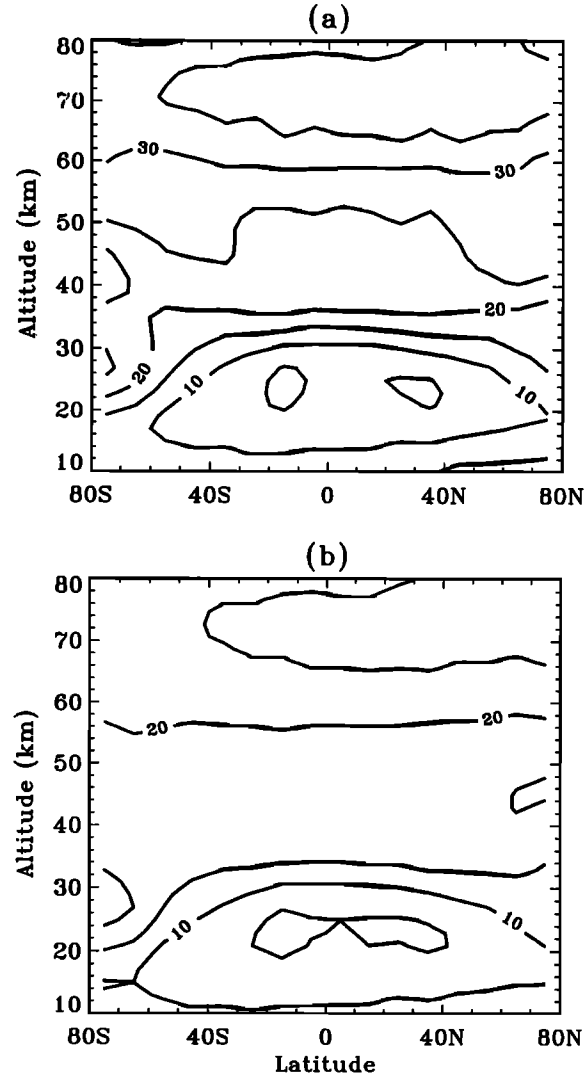

Figure 9. (a) Right and (b) left sides of the standard deviation of the ozone relative difference (percent) between its density from each GMC run of model and its nominal value.

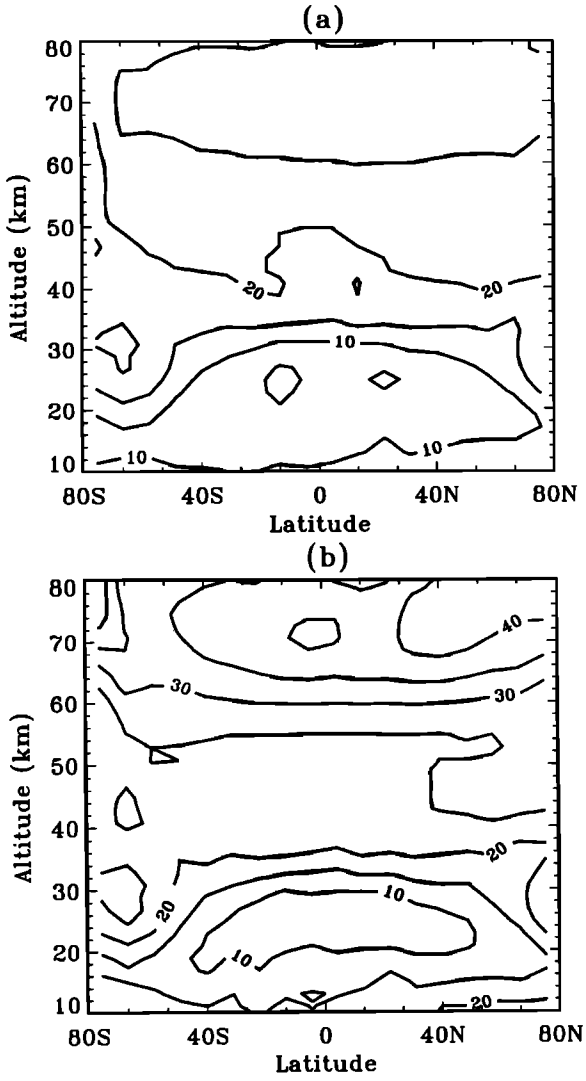

Figure 10. (a) The ozone uncertainty (%) calculated by using equation (6) for T=298 K. (b) The same as Figure 10a except for the 2-D model temperature field.

ratio of the two values at any point should be close to 1. We calculated these ratios at different latitudes and altitudes and found that the majority of the ratios do fall in a narrow belt around 1 ($\pm$0.2). The ozone concentrations derived from the sensitivity coefficients are thus not much different from the results calculated by a model run (less than 20%). This result shows that the calculated ozone concentration with respect to the input chemical reaction rates over the region (75° S–75° N, 20–70 km) is quasi-linear. The uncertainty of the ozone concentration due to the uncertainties in the reaction rates is of comparable magnitude to the ozone deficit in the upper stratosphere. It is possible that the ozone deficit results from a combination of mistakes in the reaction rates that just result in calculated ozone concentration lower than the observations.

4. Conclusion

The ozone sensitivity and uncertainty due to input chemical reaction rate uncertainties have been studied by using the GSFC 2D model. The ozone sensitivity coefficients to 96 gas phase chemical reaction rates are estimated by using a finite difference method. The sensitivity coefficients show that the ozone concentration is sensitive to the rates of only about 25 of the 96 reactions included in the 2-D model. The magnitude of the ozone sensitivity coefficients varies from 0.05 to 0.9. Ozone is most sensitive to the reaction $O+O_2+M \rightarrow O_3+M$ in both the upper stratosphere and the mesosphere over all latitudes, and the magnitude of its sensitivity coefficient varies from 0.1 to 0.9. Below 30 km at high latitudes, poleward transport in the middle stratosphere and downward motion at high latitudes increase the ozone sensitivity to this reaction. Ozone is sensitive to the NO_x reactions throughout the stratosphere, but it is sensitive to the ClO_x reactions only in a narrow region of the upper stratosphere. The latitudinal variation of the ozone sensitivity to ClO_x reactions is very similar to that of active ClO_x species. HO_x dominates above 40 km. The results of the sensitivity analysis quantify and spatially locate the importance of the various reactions and are in accord with the intuitive feeling of the atmospheric science community. While this increases our confidence that our understanding of the chemical processes regulating ozone is solid, it is important to note that the sensitivity analysis does not eliminate the possibility of missing chemical processes. The value of the ozone sensitivity coefficient to the channel $ClO+OH \rightarrow HCl+O_2$ at a 7% branching yield is about 0.1–0.2 at altitudes of 40–50 km from middle to high latitudes. Adding this channel to the 2-D model reduces the ozone sensitivity to the reactions involving ClO_x by about 0.05–0.1 at 40–50 km.

The GMC analysis is an efficient method of determining the uncertainty of the model calculated ozone arising from uncertainties in chemical reaction rates. The method reduces the cost of the Monte Carlo analysis by about a factor of 2 through a reduction in the number of necessary Monte Carlo runs of the model and employment of uncertainty estimates from the calculated sensitivity coefficients where appropriate. The GMC calculations show that the uncertainty in the calculated ozone due to the uncertainties of chemical reaction rates is at least 10–15% in the lower stratosphere and 30–35% in the mesosphere. The values of the modeled ozone uncertainty are estimated for the reaction rate uncertainties at T=298 K and are increased to 10–20% in the lower and middle stratosphere, 20–30% in the upper stratosphere, and 30–40% in the mesosphere if the realistic stratosphere and mesosphere temperature are adopted. The robust conclusion based on these results is that we cannot rule out the possibility that the ozone deficit in the upper stratosphere results from a chance combination of mistakes in the input reaction rates. The extra channel to HCl from ClO+OH reduces the ozone uncertainty by only 5–10% at 40–50 km at middle to high latitudes. This study also shows that the dependence of the model output ozone concentration on the input chemical reaction rates is approximately linear in the uncertainty region explored.

In the future, the ozone sensitivity and uncertainty to other chemical and dynamical model input parameters such as the photolysis cross section, heterogeneous reactions, solar flux, aerosol properties and abundance, vertical and meridional winds, and horizontal and vertical diffusion coefficients need to be studied. A good understanding of this source of uncertainty can result in an ability to address the ozone uncertainty due to the exclusion of important physical processes and adopting simplifying assumptions in the model.

Appendix

Chemical reactions included in the GSFC 2-D model. M is N_2 and O_2.

$O+O_2+M \rightarrow O_3+M$

$O+O_3 \rightarrow 2O_2$

$H+O_2+M \rightarrow HO_2+M$

$OH+O_3 \rightarrow HO_2+O_2$

$HO_2+O_3 \rightarrow OH+2O_2$

$ClO+HO_2 \rightarrow HOCl+O_2$

$Cl+H_2O_2 \rightarrow HCl+HO_2$

$O(^1D)+M \rightarrow O(^3P)+M$

$NO+O_3 \rightarrow NO_2+O_2$

$NO_2+O_3 \rightarrow NO_3+O_2$

$H+O_3 \rightarrow OH+O_2$

$OH+OH+M \rightarrow H_2O_2+O_2$

$OH+ClONO_2 \rightarrow NO_3+HOCl$

$CH_4+OH \rightarrow CH_3+H_2O$

$CH_3O_2+NO \rightarrow CH_3O+NO_2$

$CH_3Cl+OH \rightarrow CH_2Cl+H_2O$

$CH_3O+O_2 \rightarrow CH_2O+HO_2$

$NO_2+OH+M \rightarrow HNO_3+M$

$HO_2+HO_2 \rightarrow H_2O_2+O_2$

$N+O_2 \rightarrow NO+O$

$H_2CO+O \rightarrow HCO+OH$

$CH_3O_2+HO_2 \rightarrow CH_3OOH+O_2$

$Cl+H_2 \rightarrow HCl+H$

$Cl+O_3 \rightarrow ClO+O_2$

$ClO+O \rightarrow Cl+O_2$

$Cl+CH_4 \rightarrow HCl+CH_3$

$HCl+OH \rightarrow Cl+H_2O$

$ClO+NO \rightarrow Cl+NO_2$

$OH+H_2O_2 \rightarrow H_2O+HO_2$

$OH+H_2 \rightarrow H_2O+H$

$N_2O_5+M \rightarrow NO_2+NO_3+M$

$ClO+NO_2+M \rightarrow ClONO_2+M$

$O+H_2O2 \rightarrow OH+HO_2$

$HO_2+NO_2+M \rightarrow HO_2NO_2+M$

$O+ClONO_2 \rightarrow ClO+NO_3$

$CO+OH \rightarrow CO_2+H$

$HNO_3+OH \rightarrow NO_3+H_2O$

$NO+HO_2 \rightarrow OH+NO_2$

$H_2O+O(^1D) \rightarrow 2OH$

$OH+HO_2 \rightarrow H_2O+O_2$

$OH+O \rightarrow H+O_2$

$HO_2+O \rightarrow OH+O_2$

$NO_2+O \rightarrow NO+O_2$

$NO_2+O+M \rightarrow NO_3+M$

$N_2O+O(^1D) \rightarrow 2NO$

$NO_2+NO_3+M \rightarrow N_2O_5+M$

$N+NO \rightarrow N_2+O$

$H_2+O(^1D) \rightarrow OH+H$

$CH_4+O(^1D) \rightarrow OH+CH_3$

$CH_3+O_2+M \rightarrow CH_3O_2+M$

$H_2CO+OH \rightarrow H_2O+HCO$

$HCO+O_2 \rightarrow CO+HO_2$

$Cl+HO_2 \rightarrow HCl+O_2$

$CCl_4+O(^1D) \rightarrow 4Cl+products$

$OH+HO_2NO_2 \rightarrow H_2O+O_2+NO_2$

$CH_4+O(^1D) \rightarrow H_2CO+H_2$

$OH+CH_3OOH \rightarrow H_2O+CH_3O_2$

$OH+OH \rightarrow H_2O+O$

$ClO+OH \rightarrow Cl+HO_2$

$HOCl+OH \rightarrow H_2O+ClO$

$Cl+H_2CO \rightarrow HCl+HCO$

$HO_2+HO_2+M \rightarrow H_2O_2+O_2+M$

$CFClO+O(^1D) \rightarrow products$

$CF_2O+O(^1D) \rightarrow products$

$Cl+HO_2 \rightarrow OH+ClO$

$N+OH \rightarrow NO+H$

$HO_2NO_2+M \rightarrow HO_2+NO_2+M$

$H+HO_2 \rightarrow H_2+O_2$

$H+HO_2 \rightarrow H_2O+O$

$H+HO_2 \rightarrow OH+OH$

$NO+NO_3 \rightarrow 2NO_2$

$OH+CH_3CCl_3 \rightarrow 3Cl$

$NO+O+M \rightarrow NO_2+M$

$N_2O+O(^1D) \rightarrow N_2+O_2$

$O(^1D)+CF_2Cl_2 \rightarrow Cl+ClO+frag$

$N+NO_2 \rightarrow N_2O+M$

$O(^1D)+N_2+M \rightarrow N_2O+M$

$O(^1D)+CFCl_3 \rightarrow 2Cl+ClO+frag$

$O(^1D)+decay \rightarrow O+h\upsilon$

$O+O+M \rightarrow O_2+M$

$Br+O_3 \rightarrow BrO+O_2$

$Br+HO_2 \rightarrow HBr+O_2$

$BrO+ClO \rightarrow Br+Cl+O_2$

$BrO+BrO \rightarrow Br+Br+O_2$

$OH+HBr \rightarrow H_2O+Br$

$BrO+NO_2+M \rightarrow BrONO_2+M$

$CH_3Br+OH \rightarrow Br+products$

$CHClF_2+OH \rightarrow Cl+products$

$C_2Cl_3F_3+O(^1D) \rightarrow 3Cl+products$

$C_2Cl_2F_4+O(^1D) \rightarrow 2Cl+products$

$C_2ClF_5+O(^1D) \rightarrow Cl+products$

$ClO+ClO+M \rightarrow Cl_2O_2+M$

$BrO+ClO \rightarrow Br+OClO$

$BrO+ClO \rightarrow Br+ClOO$

$BrO+ClO \rightarrow BrCl+O_2$

$Cl_2O_2+M \rightarrow ClO+ClO$

Acknowledgments. The authors acknowledge support from the NASA Headquarters Atmospheric Chemistry Modeling and Analysis Program for this project. One of the authors (J.S.) acknowledges support from DOE. We also acknowledge valuable discussion with C. Kolb at the inception of this project.

References

Andronova, N. G., and M. E. Schlesinger, The application of cause-and-effect analysis to mathematical models of geophysical phenomena, 1. Formulation and sensitivity analysis, *J. Geophys. Res.*, *96*, 941–946, 1991.

Brasseur, G. and C. Granier, Mount Pinatubo aerosols, chlorofluorocarbons, and ozone depletion, *Science*, *257*, 1239–1242, 1992.

Brasseur, G., M. H. Hitchman, S. Walters, M. Dymek, E. Falise, and M. Pirre, An interactive chemical-dynamical radiative two-dimensional model of the middle atmosphere, *J. Geophys. Res.*, 95, 5639–5655, 1990.

Butler, D. M., The uncertainty in ozone calculations by a stratospheric photochemistry model, *Geophys. Res. Lett.*, 5, 769–772, 1978.

Chandra, S., C. H. Jackman, A. R. Douglass, E. L. Fleming, and D. B. Considine, Chlorine catalyzed destruction of ozone: Implications for ozone variability in the upper stratosphere, *Geophys. Res. Lett.*, *20*, 351–354, 1993.

Considine, D. B., A. R. Douglass, and C. H. Jackman, Effects of a polar stratospheric cloud parameterization on ozone depletion due to stratospheric aircraft in a two-dimensional model, *J. Geophys. Res.*, *99*, 18,879–18,894, 1994.

DeMore, W. B., S. P. Sander, D. M. Golden, R. F. Hampson, M. J. Kurylo, C. J. Howard, A. R. Ravishankara, C. E. Kolb, and M. J. Molona, Chemical kinetics and photochemical data for use in stratospheric modeling, Evaluation number 10, *JPL Publ.*, *92–20*, 1992.

Dopplick, T. G., The heat budget, in *The General Circulation of the Tropical Atmosphere and Interactions With Extratropical Latitudes*, vol. 2, edited by R. E. Newell, J. W. Kidson, D. G. Vincent, and C. J. Boer, pp. 27–94, MIT Press, Cambridge, Mass., 1974.

Dopplick, T. G., Radiative heating of the global atmosphere: Corrigendum, *J. Atmos. Sci.*, *36*, 1812–1817, 1979.

Douglass, A. R., and R. S. Stolarski, The use of atmospheric measurements to constrain model predictions of ozone change from chlorine perturbations, *J. Geophys. Res.*, *92*, 6662–6674, 1987.

Douglass, A. R., C. H. Jackman, and R. S. Storlarski, Comparison of model results transporting the odd nitrogen family with the results transporting separate odd nitrogen species, *J. Geophys. Res.*, *94*, 9862–9872, 1989.

Dunkerton, T., On the mean meridional mass motions of the stratosphere and mesosphere, *J. Atmos. Sci.*, *35*, 2325–2333, 1978.

Fleming, E. L., S. Chandra, C. H. Jackman, D. B. Considine, and A. R. Douglass, The middle atmospheric response to short and long term solar UV variations: analysis of observations and 2D model results, *J. Atmos. and Terr. Phys. 57*, 333–365, 1995.

Garcia, R. R., and S. Solomon, A new numerical model of the middle atmosphere, 2, Ozone and related species, *J. Geophys. Res.*, *99*, 12,937–12,951, 1994.

Garcia, R. R., F. Stordal, S. Solomon, and J. F. Kiehl, A new numerical model of the middle atmosphere, 1, Dynamics and transport of tropospheric source gases, *J. Geophys. Res.*, *97*, 12,967–12,991, 1992.

Hanson, D. R., and A. R. Ravishankara, Reaction of $ClONO_2$ with HCl on NAT, NAD, and frozen sulfuric acid and hydrolysis of N_2O_5 and $ClONO_2$ on frozen sulfuric acid, *J. Geophys. Res.*, *98*, 22,931–22,936, 1993.

Hanson, D. R., and A. R. Ravishankara, Reactive uptake of $ClONO_2$ onto sulfuric acid due to reactions with HCl and H_2O, *J. Phys. Chem.*, *98*, 5728–5735, 1994.

Jackman, C. H., A. R. Douglass, R. B. Rood, R. D. McPeters, and P. E. Meade, Effect of solar proton events on the middle atmosphere during the past two solar cycles as computed using a two-dimensional model, *J. Geophys. Res.*, *95*, 7417–7428, 1990.

Kaye, J. A. and C. H. Jackman, Concentrations and uncertainties of stratospheric trace species inferred from Limb Infrared Monitor of the Stratosphere data 1. Methodology and application to OH and HO_2, *J. Geophys. Res.*, *91*, 1117–1135, 1986a.

Kaye, J. A., and C. H. Jackman, Concentrations and uncertainties of stratospheric trace species inferred from Limb Infrared Monitor of the Stratosphere data, 2, Monthly averaged OH, HO_2, H_2O_2, and HO_2NO_2, *J. Geophys. Res.*, *91*, 1137–1152, 1986b.

McElroy, M. B. , and R. J. Salawitch, Changing composition of the global stratosphere, *Science*, *243*, 763–770, 1989.

Minschwaner, K., R. J. Salawitch, and M. B. McElroy, Absorption of solar radiation by O_2: Implications for O_3 and lifetimes of N_2O, $CFCl_3$, and CF_2Cl_2 *J. Geophys. Res.*, *98*, 10,543–10,561, 1993.

National Research Council (NRC) panel on atmospheric Chemistry, Halocarbons: Effects on stratospheric ozone, pp.352, Natl. Acad. of Sci., Washington, D. C., Sept. 1976.

Prather, M. J., Numerical advection by conservation of second-order moments, *J. Geophys. Res.*, *91*, 6671–6681, 1986.

Rosenfield, J. E., M. R. Schoeberl, and M. A. Geller, A computation of the stratospheric diabatic residual circulation using an accurate radiative transfer model, *J. Atmos. Sci.*, *44*, 859–876, 1987.

Schneider, H. R., M. K. W. Ko, R. L. Shia, and N. D. Sza, A two dimensional model with coupled dynamics, radiative transfer, and

photochemistry, 2, Assessment of the response of stratospheric ozone to increased levels of CO_2, N_2O, CH_4, and CFC, *J. Geophys. Res., 98*, 20,441–20,449, 1993.

Shorter, J. A, and H. A. Rabitz, Risk analysis by the guided Monte Carlo technique, *J. Statist. Comput. Simul.*, in press, 1997..

Stolarski, R. S., Uncertainty and sensitivity studies of stratospheric photochemistry, in *Proceeding of the NATO Advanced Study Institute on Atmospheric Ozone: Its Variations and Human Influences,* edited by A. C. Aikin, Rep. FAA-EE-80-20., pp. 865–876, U. S. Dep. of Transp., Washington D.C., 1980.

Stolarski, R. S., and A. R. Douglass, Sensitivity of an atmospheric photochemistry model to chlorine perturbations including consideration of uncertainty propagation, *J. Geophys. Res., 91*, 7853–7864, 1986.

Stolarski, R. S. , D. M. Bulter, and R. D. Rundel, Uncertainty propagation in a stratospheric model, 2, Monte Carlo analysis of imprecisions due to reaction rates, *J. Geophys. Res., 83*, 3074–3078, 1978.

Tabazadeh, A., and R. P. Turco, A model for heterogeneous chemical processes on the surfaces of ice and nitric acid trihydrate particles, *J. Geophys. Res., 98*, 12,727–12,740, 1993.

World Meteorological Organization, (WMO), Scientific Assessment of Stratospheric Ozone: 1994, *Rep. 37*, Global Ozone Res. and Monit. Proj., Geneva, 1994.

L. Chen, Advanced Study Program, National Center for Atmospheric Research, P.O. Box 3000, Boulder, CO 80307. (e-mail: chenli@acd.ucar.edu)

D.B. Considine and C.H. Jackman, Atmospheric Chemistry and Dynamics Branch, NASA Goddard Space Flight Center, Greenbelt, MD 20771.

H. Rabitz, Department of Chemistry, Princeton University, Princeton, NJ 08544

J.A. Shorter, Atmospheric and Space Science Division, Mission Research Corporation, Nashua, NH 03062.

(Received August 20, 1996; revised January 16, 1997;
accepted January 17, 1997.)